Giant Momentum Coupling Coefficients from Nanoscale Laser-initiated Exothermic Compounds

Claude R. Phipps[*] and James R. Luke[†]
Photonic Associates, LLC, Santa Fe, NM 87508

Wesley D. Helgeson[‡]
NMT/IERA, Albuquerque, NM 87106

Darren Naud and Michael Hiskey[§]
Los Alamos National Laboratory, Los Alamos, NM 87545

Lukas Urech[**], Thomas Lippert[††] and Alexander Wokaun[‡‡]
Paul Scherrer Institut, Villigen PSI, Switzerland

We report here on results obtained with laser-initiated micro-propellants, such as PVN, PVC, GAP, NC, and mixtures of these. All samples were doped with a laser absorbing component. In some cases, this was carbon nanopearls with 10nm mean diameter, while, in others, it was a carbon-based ink with μm-size particles. We also report results of performance tests for absorbers tuned to the 935-nm laser wavelength.

Nomenclature

C_m	=	laser momentum coupling coefficient
CA	=	cellulose acetate
E	=	short for "10^"
EFL	=	effective focal length
eV	=	electron-volt
F	=	thrust
FEP	=	fluoroethylene polymer
g_o	=	acceleration of gravity at Earth's surface
GAP	=	glycidyl azide polymer
I	=	laser intensity on target
I_p	=	plasma formation threshold intensity
I_{sp}	=	specific impulse
K	=	DuPont Kapton™ polyimide resin
NC	=	nitrocellulose
$<P>$	=	average incident laser power

[*] President and General Partner, 200A Ojo de la Vaca Road, crphipps@aol.com. Member AIAA.
[†] Senior Research Staff Member and Partner, 200A Ojo de la Vaca Road.
[‡] Senior Research Associate, 901 University Blvd SE.
[§] Research Staff Member, P.O. Box 1663.
[**] Research Staff Member, Materials Group
[††] Head, Materials Group
[‡‡] Head, General Energy Research Department; also Professor, Chemistry Department, ETH Zürich

Report Documentation Page

Form Approved
OMB No. 0704-0188

1. REPORT DATE	2. REPORT TYPE	3. DATES COVERED
APR 2005		**-**

4. TITLE AND SUBTITLE	5a. CONTRACT NUMBER
Giant Momentum Coupling Coefficients from Nanoscale Laser-initiated Exothermic Compounds	**FA9300-04-C-0030**
	5b. GRANT NUMBER
	5c. PROGRAM ELEMENT NUMBER
6. AUTHOR(S)	5d. PROJECT NUMBER
Claude Phipps; James Luke; Wesley Helgeson; Darren Naud; Michael Hiskey	**BMSB**
	5e. TASK NUMBER **R3LA**
	5f. WORK UNIT NUMBER
7. PERFORMING ORGANIZATION NAME(S) AND ADDRESS(ES)	8. PERFORMING ORGANIZATION REPORT NUMBER
Photonic Associates, LLC,200 Ojo de la Vaca Road,Santa Fe,NM,87508	
9. SPONSORING/MONITORING AGENCY NAME(S) AND ADDRESS(ES)	10. SPONSOR/MONITOR'S ACRONYM(S)
	11. SPONSOR/MONITOR'S REPORT NUMBER(S)

12. DISTRIBUTION/AVAILABILITY STATEMENT
Approved for public release; distribution unlimited

13. SUPPLEMENTARY NOTES

14. ABSTRACT
We report here on results obtained with laser-initiated micro-propellants, such as PVN PVC, GAP, NC, and mixtures of these. All samples were doped with a laser absorbing component. In some cases, this was carbon nanopearls with 10nm mean diameter, while, in others, it was a carbon-based ink with µm-size particles. We also report results of performance tests for absorbers tuned to the 935-nm laser wavelength.

15. SUBJECT TERMS

16. SECURITY CLASSIFICATION OF:			17. LIMITATION OF ABSTRACT	18. NUMBER OF PAGES	19a. NAME OF RESPONSIBLE PERSON
a. REPORT	b. ABSTRACT	c. THIS PAGE			
unclassified	**unclassified**	**unclassified**		**5**	

PVC = polyvinyl chloride
PVN = polyvinyl nitrate
*Q** = specific ablation energy
T = temperature
v_E = exhaust velocity
W = laser pulse energy incident on test sample
Δm = ablated mass
η_{AB} = ablation efficiency
τ = laser pulse duration

I. Introduction

The maximum specific impulse available from chemical reactions is about 500s, limited by the heat of formation. For example, the heat of formation for hydrogen-oxygen combustion, one of the hottest chemical reactions, is 57.8 kcal/mole[1]. This translates to a reaction temperature of 2.91E4K, for which the most probable thermal velocity $(2kT/m_E)^{0.5}$ = 5.17 km/s, or I_{sp}= 527 s. However, for example, the Space Shuttle's main engine can produce only 465 s (v_E= 4.56 km/s), because of inefficiencies inherent in the engine[2]. This limit is fundamental, and will not change with improvements in engine materials. Larger I_{sp} values (v_E >> 5km/s) are accessible only by laser ablation, where temperatures can be more than 1E6K for ns-duration pulses, or some other non-chemical process such as ion drives. Specific impulse I_{sp} up to 7600s has been measured[3] with 20ns-duration pulses from an ordinary KrF laser illuminating Al. This I_{sp} corresponds to T = 9.1E6 K (780 eV). By combining these two effects, i.e., not only initiating the reaction, but adding significant energy with very intense pulses of laser illumination, the potential exists for attaining combinations of C_m and I_{sp} in which I_{sp} still exceeds what is available from the chemistry alone, and in which η_{AB} >1. In the work reported here, which deals with ms-duration laser pulses at the modest intensities available from multi-mode diode lasers, we do not expect to see I_{sp} > 500s, but do expect η_{AB}>1 and the distinct advantage of programmable, discrete target addressability.

II. Definition of Terms

For the sake of simplicity, we will consider a monoenergetic laser-produced plasma jet with exhaust velocity v_E. We have shown[3,4] that this approximation will not introduce large errors [$\langle v^2\rangle/\langle v\rangle^2 \approx 1.15$] for typical laser-produced plasma jets, and the principal points we want to make here will be made more transparently using that assumption. We define C_m as follows:

$$C_m = F/\langle P\rangle = \Delta m v_E/W. \quad (1)$$

In the ablation process, Q* joules of laser light are consumed per kg of ablated mass, and C_m units of impulse $\Delta m v_E$ are produced. The product of C_m and Q* is the exhaust velocity v_E of the ablation stream, given the monoenergetic assumption. This can be seen from the definitions of C_m and Q*:

$$C_m Q^* = (\Delta m v_E/W)(W/\Delta m) = v_E \quad (2)$$

independent of the ablation efficiency. If for example, a significant amount of the incident energy is absorbed as heat in the target substrate rather than producing material ejection, Q* will be higher, but C_m will be proportionately lower, giving the same velocity in the end. In propulsion work, "specific impulse" I_{sp} is customary notation for v_E/g_o. In this work, we define I_{sp} as

$$I_{sp} = C_m Q^*/g_o \quad (3)$$

Energy conservation prevents C_m and I_{sp} from being arbitrary. Increasing one decreases the other. Energy conservation requires that several constant product relationships exist:

$$2\eta_{AB} = \Delta m v_E^2/W = C_m^2 Q^* = g_o C_m I_{sp} = C_m v_E. \quad (4)$$

In Eq. (3), we introduce the ablation efficiency parameter, η_{AB}, the ratio of exhaust kinetic energy to incident laser energy W. The definition allows $\eta_{AB} > 1$ for exothermic targets.

For nonexothermic targets, $\eta_{AB} \leq 1$, and the product

$$C_m I_{sp} \leq 2/g_o = 0.204. \quad (5)$$

Plasma formation threshold is approximately given by[5]

$$I_p = 240/\tau^{0.55} MW/m^2. \quad (6)$$

Eq. (6) is a useful guide valid to within factors of 2 for ms to sub-ns pulse durations, for all surface absorbing materials in vacuum, and for visible to infrared wavelengths. It is also a useful guide for predicting plasma initiation in confined ablation.

III. Target Preparation

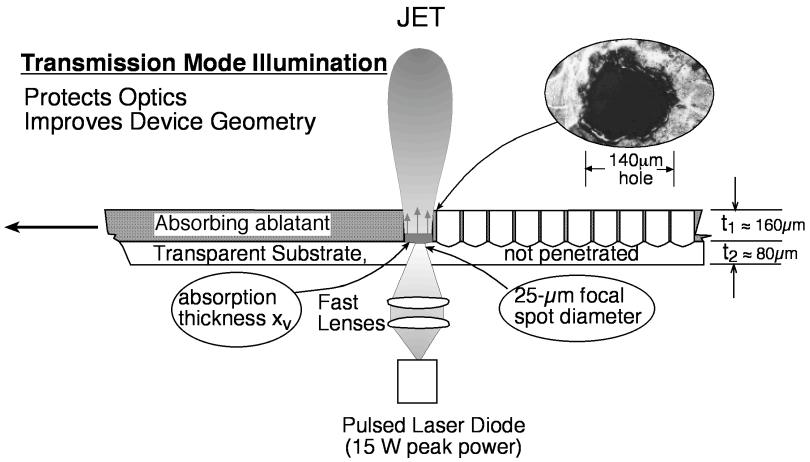

Figure 1. Schematic of Target Tapes. Each laser pulse passes through the transparent substrate and creates a detonation which begins at the interface between it and an absorbing ablatant layer. The detonation expands to produce the jet. The transparent substrate is not physically penetrated, although some of it may also ablate.

Ablation targets for tests were made in a tape format using a variety of transparent supporting substrates and ablative coatings [Fig.1]. Substrates were chosen for transparency, low outgassing and high optical damage resistance. We found that these requirements were often difficult to satisfy simultaneously. For example, Kapton™ polyimide resin has excellent toughness and outgassing properties, but lower optical damage resistance and adhesivity for some target materials, compared to cellulose acetate. The polyimide has lower damage resistance because of its greater absorptivity at our 935-nm operating wavelength. Among the materials considered for substrates, only cellulose acetate and FEP were excellent in regard to optical damage resistance. However FEP had the added problem of very poor adhesion to most coatings other than vapor-deposited aluminum, so we settled on cellulose acetate as the best substrates for general use, and polyimide for cases in which the coating application process involves solvents not tolerated by cellulose acetate. Tape substrate thickness ranged from 75 to 125μm. Coatings ranged from 60μm to 370μm.

Coating materials were mixed with a Cole-Parmer A-04737 homogenizer.

Ablative coatings for tapes were usually applied as a spray of the coating material diluted in, e.g., n-butyl acetate, in increments of 5μm, to attain an ideal total thickness of order 70μm. In some cases, coatings were applied in one go using a draw-blade applicator.

Laser ablatant materials and substrates are listed in Table 1. All proportions are by weight. “Ink” in the Table is the black material dissolved from commercial electric typewriter foil ribbon.

IV. Experimental Setup

A. Ablator Test Device

Figure 2 shows the device used to illuminate the target tapes.

One to four repetitively-pulsed, fiber-coupled JDSU type 6380-A/L2 laser diodes inside the device drive the ablation of the fuel tape. Each of these are capable of <P> = 2.5W output at 910-920 nm wavelength with input current and voltage of 3.37A and 1.71V, giving 43% electrical efficiency at this output level. At 1ms pulse duration, we determined that these could achieve peak delivered power output of 4.75W at 10% duty cycle without damage. The ends of the four 100-μm-core-diameter fibers were stripped of their buffer layers for closest spacing, and mounted in a fiber vise. Their light output was collimated with a Lightpath, Inc. GPX5-5 axially graded refractive index aspheric lens and focused with a Thorlabs C330-TM-B aspheric. The EFL's of the two lenses are 5.16 mm and 3.10 mm, respectively. Both lenses are AR-coated. Intensity on target is about 30GW/m^2 when 15W peak are incident from all four lasers. A stepper motor drives the closed-loop fuel tape in the longitudinal direction at speeds of 5 to 20 mm/s. A second stepper motor slowly advances the beam delivery system (fiber ends and two lenses) across the tape at a rate of one track width per revolution of the tape loop, resulting in a continuous helical path that eventually accesses the entire tape.

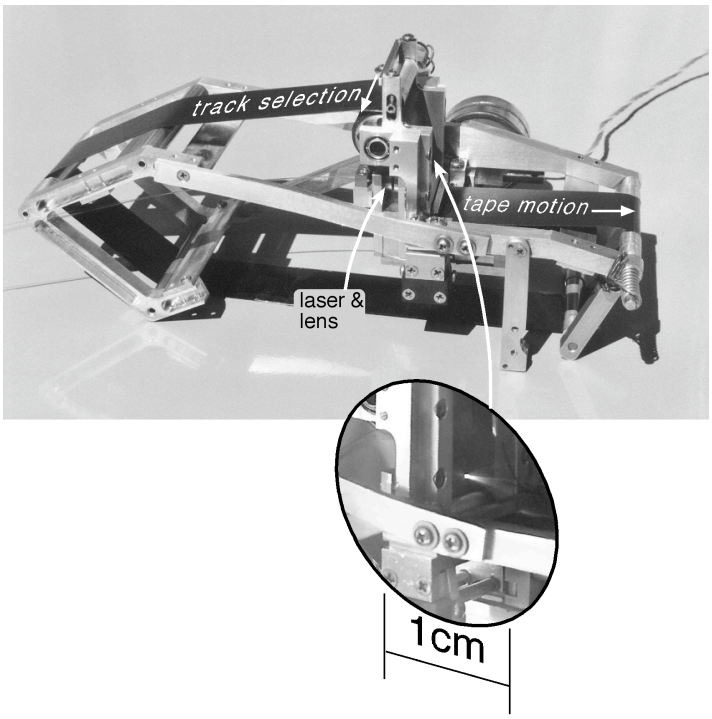

Figure 2. Ablation tape test unit. The inset shows the laser-produced plasma jet.

B. Micronewton Test Stand

The test unit was mounted to one end of a counterbalanced bar suspended by a 250-μm steel fiber inside a vacuum chamber[6]. Thrust F generated by the test unit was determined by measuring the rotation of the bar. Ablation mass loss Δm was determined by weighing the ablation test tape before and after a test run using a microgram Mettler balance. Ambient pressure during tests was typically 50μtorr.

To eliminate external torsion inputs to the thrust measurement, power is supplied to the testbed thruster by onboard Li-ion batteries (which, with electronics, constitute the counterbalance), and test unit operation is controlled by an external computer via an optical link.

Since the publication of reference 6, these measures have improved the resolution of our torsion pendulum to ±2μN [Figure 3].

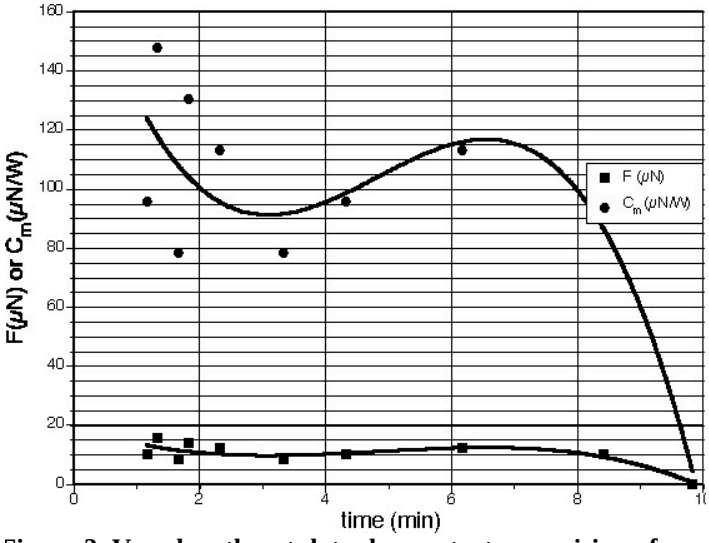

Figure 3. Very low thrust data demonstrates precision of our μN thrust stand. The scatter is not due to measurement error, but rather the periodic motion of the torsion balance. The solid lines are a third-degree polynomial fit to the data. Precision of the thrust stand with a simple probe-laser readout is ±2μN. Even better precision has been demonstrated with an interferometric readout, and will be reported in a subsequent paper.

V. Results

Results we obtained are given in Table 2.

VI. Conclusion

Our results showed the largest coupling coefficient C_m ever reported for some target materials, almost 2mN/W.

As expected from its definition, η_{AB}>1 for the GAP test samples, but much lower for the less exothermic materials.

Table 1. Laser Ablatant Materials

Ablator	Absorber	Substrate
PVN	10% carbon nanopearls	CA
PVC	5% ink	CA
GAP	carbon nanopearls	K
GAP	5% ink	K
GAP	1% Epolin 2057 935-nm absorber	K
PVN	1% Epolin 2057 935-nm absorber	K
NC	2% carbon nanopearls	CA

The specific impulse values in the table, computed from measured mass loss of the ablated tapes, correspond to exhaust velocities up to 2.5km/s. These values do not exceed what is available from chemistry. The advantage of using the combination of laser and chemical energy in the present work is discrete, programmable thrust output.

We reported ±2μN sensitivity in our torsion-balance-based thrust stand, a figure which is substantially improved relative to earlier reports.[6]

Table 2. Results of Measurements

Ablator	$\mathbf{I}$(MW/m^2)	$\boldsymbol{\tau}$(ms)	$\mathbf{C_m}$(μN/W)	$\mathbf{F}$(μN)	$\mathbf{I_{sp}}$(s)	$\boldsymbol{\eta_{AB}}$(%)
PVN/10% carbon nanopearls	403	1	310	113	137	21
PVN/10% ink	403	1	256	94	155	19
PVN/1% Epolin 2057	175	1	103	35	76	4
GAP/ carbon nanopearls	175	1	1960	392	188	181
GAP/5% ink	150	1	1970	394	190	183
GAP/1% Epolin 2057	230	1	1574	167	256	198
PVC/5% ink	570	2.5	94	137	189	8.7
NC/2% carbon nanopearls	400	1	471	179	183	42

In nearly identical circumstances, nanopearl carbon as a laser absorber gave similar or better performance compared to ink (which contains μm- rather than nm-size particulates), while the tuned absorber dye gave similar or somewhat worse performance. Although the advantage is slight, we saw a definite benefit to using nanosize absorbing particles. We believe this is not due to better light-absorbing efficiency of nanosize particulates, nor, for ms-duration pulses to higher transient temperatures, but rather to more intimate interaction with the exothermic components of the absorbing mix.

References

1 Weast, R. (ed.), *CRC Handbook of Chemistry and Physics*, Chemical Rubber Publishing Co, Cleveland, 1978, p D-71

[2] Johnson, R.D. & Holbrow, C. (eds.), *Space Settlements, a Design Study*, NASA report SP-413, 1977

[3] Phipps, C. and Michaelis, M., "Laser Impulse Space Propulsion", *Journal of. Laser and Particle Beams* **12** no. 1, 1994, pp. 23-54

[4] Phipps, C., Reilly, J. and Campbell, J., "Optimum Parameters for Laser-launching Objects into Low Earth Orbit", *J. Laser and Particle Beams*, **18** no. 4, 2000, pp. 661-695

[5] Phipps, C. R. and Luke, J. R., "Diode Laser-driven Microthrusters: A new departure for micropropulsion," *AIAA Journal* **40** no. 2 2002, pp. 310-318

[6] Phipps, C. , Luke, J., Lippert, T., Hauer, M. and Wokaun, A., "Micropropulsion using a Laser Ablation Jet," *J. Propulsion and Power*, **20** no. 6, 2004, pp. 1000-1011